Environ. Sci. Technol. **2000**, *34,* 5215−5221

Optimal Design of an In Situ Fe(II) Barrier: Transport Limited Reoxidation

ASHOK CHILAKAPATI*
Xerago LLC, 2535 Kettner Boulevard, Suite 2A2, San Diego, California 92101

MARK WILLIAMS, STEVE YABUSAKI, CHARLIE COLE, AND JIM SZECSODY
Pacific Northwest Laboratory, Richland, Washington 99352

Harmful contaminants such as Cr(VI) and TCE can be removed from groundwater by reactions with chemically reduced subsurface sediments. This paper studies the optimal selection of the number of wells, the injection rate, and the number of regenerations of a large-scale Fe(II) barrier for Cr(VI) remediation at Hanford, WA. The process model consists of two parts: (a) the creation of the Fe(II) barrier by the injection of a dithionite reagent and (b) the reoxidation of the barrier by Cr(VI) and oxygen in the invading groundwater. The solution to the process model is used to develop the total cost as a function of the design variables. This cost model is applied to the Cr(VI) contamination at Hanford to obtain the optimal design configuration and its sensitivity to cost and process uncertainties.

Introduction

Permeable reactive barriers have attracted much attention because of their potential for cost-effective in situ treatment of many redox-sensitive groundwater contaminants (*1*). Zero-valent iron has been shown to be an effective reductant for nitro aromatic compounds (*2*), hexavalent chromium (*3*), and TCE (*4*). The effectiveness of ferrous iron for TCE degradation and Cr(VI) removal from aqueous phase is known (*5*−*7*). Application of a zero-valent iron barrier has been reported (*8*) for Cr(VI) remediation where the barrier was created by trench-and-fill techniques. Amonette et al. (*9*) have developed the In Situ Redox Manipulation (ISRM) approach where a buffered dithionite reagent is injected to reduce naturally occurring ferric iron in the sediments to ferrous iron (U.S. Patent 5,783,088). Injectable barriers have since been successfully demonstrated at bench and intermediate scales (*10*) and recently in proof-of-principle field tests (*11*) for Cr(VI) remediation. This paper is concerned with the large-scale field implementation of the ISRM technology for Cr(VI) plumes at the Hanford site. To that end, simplified descriptions of the physics (e.g., homogeneous formation) and chemistry (e.g., a total of four reactions describe the pH-buffered redox process) deemed appropriate to the field scale are employed. The focus is on the development of an optimal deployment strategy that minimizes the total cost of operation.

ISRM Approach. The ISRM approach is based on the reduction of iron(III) oxides and structural Fe(III) within the clay minerals by the dithionite ion, which is a strong reductant in basic solutions. Experimental evidence indicates that while the dithionite treatment dissolves away the amorphous iron oxides, the structural iron within the clay minerals stays largely intact in the sediment forming an Fe(II) barrier. Furthermore, the dissolved Fe(II) readsorbs on to the sediment. Amonette et al. (*9*) have described the aqueous chemistry of the dithionite ion and the transfer of electrons to Fe(III) in the solid phase that forms Fe(II). Each dithionite ion produces two sulfoxyl radicals that are available to reduce Fe(III) to Fe(II) (the desired reaction). But they also undergo a sediment-catalyzed disproportionation, leading to a wastage of the injected reagent:

$$S_2O_4^{2-} + 2Fe(III)(s) + 2H_2O \xrightarrow{k_1} 2SO_3^{2-} + 2Fe(II)(s) + 4H^+ \quad \text{redox} \quad (1)$$

$$2S_2O_4^{2-} + H_2O \xrightarrow{k_2} 2HSO_3^- + S_2O_3^{2-} \quad \text{disproportionation} \quad (2)$$

Because the stability of the dithionite reagent is enhanced at high pH, the reagent consisted of a potassium carbonate/bicarbonate buffer (pH 11) at four times the concentration of sodium dithionite. The aquifer sediment has a relatively small buffering capacity. The influence of sediment buffering versus added carbonate buffer was addressed by Szecsody et al. (*5*). Sediment buffering at the high 0.06 mol/L aqueous concentrations of dithionite added contributes little during the several hours time scale of reduction reactions, so carbonate/bicarbonate buffering at the stoichiometric ratio of 4× to dithionite is necessary to maintain the high pH. Not maintaining the pH has additional secondary effects in that iron reduction is slower at more neutral pH and dithionite disproportionation is faster (i.e., the process is less efficient). Both reactions have a finite rate and an approximate first-order dependence on the dithionite concentration (*9*, *10*). k_1 (1/h) and k_2 (1/h) are the first-order rate constants associated with the eqs 1 and 2. Batch and column experiments with Hanford sediments indicated that the redox reaction has an approximate half-life of 5 h whereas the disproportionation is slower with a half-life of 18 h.

The Fe(II) barrier created by the dithionite injection will gradually be reoxidized to Fe(III). The primary contributors to the reoxidation are the dissolved oxygen if present and the target contaminant(s) in the plume passing through the barrier. There will also be some "loss" of the reductive capacity due to recharge, water table fluctuations that can trap air bubbles (*12*, *13*) providing a source of oxygen, the diffusion of oxygen from the vadose zone, and perhaps also from the bottom confining layer. The loss of reductive capacity is somewhat difficult to quantify as the different mechanisms for this loss are highly site dependent. The loss would be more significant when recharge is large, when the aquifer is shallow, or when the water table fluctuations are rapid (relative to the years of lifetime typically expected of the barrier). Each mole of O_2 oxidizes 4 mol ($F_o = 4$) of Fe(II) according to the reversible reaction:

$$4Fe(II) + O_2 + 4H^+ \leftrightarrow 4Fe(III) + 2H_2O \quad (3)$$

whereas each mole of Cr(VI) oxidizes 3 mol ($F_c = 3$) of Fe(II) according to the essentially irreversible reaction:

* Corresponding author e-mail: achilakapati@xerago.com; fax: (619)231-6188; phone: (619)231-5987.

10.1021/es000920h CCC: $19.00
Published on Web 11/16/2000

$$3Fe(II)(s) + HCrO_4^- + 4H^+ \rightarrow \{Fe,Cr\}(OH)_3\downarrow + 3Fe(III)(s) + 2H_2O \quad (4)$$

leading to the precipitate {Fe, Cr}$(OH)_3$. Under most groundwater and aquifer conditions, the solubility of {Fe, Cr}$(OH)_3$ is quite small (*6*, *7*) and reoxidation is unlikely (*14*, *15*) so that the Fe(II) barrier is effective at sequestering and immobilizing Cr(VI). The oxidation of Fe(II) by the dissolved oxygen and the precipitation of chromium hydroxide are fast enough (as compared to the transport time scales) to be considered instantaneous.

Hanford Site. Following the successful proof-of-principle test at the 100-H area of the Hanford site (*11*), a large-scale Fe(II) barrier for Cr(VI) remediation is being deployed in the 100-D area of the Hanford site for the remediation of Cr(VI) contamination in groundwater. The site is located in the northern portion of the site, approximately 500 ft from the Columbia River. The aquifer is composed of fluvial sandy gravels in the Ringold formation that is above the much deeper confined basalt aquifer. It is 15 ft thick and bounded on the bottom by a laterally extensive silt/clay layer. Parallel to the river, the plume is over 2000 ft wide. The distance from the river to the probable source area is 2500 ft. The source is not well characterized so that there are large uncertainties in the probable duration of the plume being fed by the source. The plume has an average Cr(VI) concentration, C_c, of 1 mg/L and is nearly saturated with dissolved oxygen ($C_o = 8$ mg/L). The groundwater is calcium bicarbonate water with a pH of 7.7. The groundwater flow direction and magnitudes are influenced by the Columbia River stage. Under normal conditions, groundwater flow directions are toward the river with a pore velocity of about 1 ft/day. The average hydraulic conductivity of the aquifer is 54 ft/day. The recharge at the site is less than 1 cm/yr, and the water table fluctuations are a few inches over the 15 ft aquifer.

The unsaturated reactive transport of gaseous and dissolved oxygen is numerically solved (*16*) to estimate the total vertical influx of oxygen due to recharge and diffusion. It turns out to be rather small at about 0.0025 mol/m^2 per year. Because each mole of oxygen oxidizes 4 mol of Fe(II), the loss of reductive capacity over a 10-year period would be 0.1 mol/m^2. At Hanford, the initially available Fe(II) over the full vertical extent of the barrier is about 113.7 mol/m^2 [Fe(II) solid concentration of 177.57 mol/m^3 of pore-space multiplied by the height 4.572 m and porosity 0.14], which is over 4 orders of magnitude larger.

Barrier Design. The width of the barrier is determined by requiring that the total treatment capacity (i.e., the accessible, reducible Fe(III) content) of the barrier be sufficient to consume the oxidizing capacity of the plume migrating through the zone. The oxidizing capacity of the plume results from both the Cr(VI) contaminant and the dissolved oxygen. Long and/or highly concentrated plumes require wider barriers for complete treatment. Because the creation of wide barriers from central injection wells is often inefficient, it is advantageous to create a barrier of smaller width but to regenerate it periodically. The number of regenerations controls the required barrier width, the injection rate plays a key role in creating the barrier with that width, and the number of wells is the key variable in building a barrier that spans the entire lateral extent of the plume. Given the generally large costs of field-scale remediation systems, the goal of this paper is to present an approach to pick these three design variables (the injection rate, the number of wells, and the number of regenerations) to minimize the total cost of operation. The main components of the total cost are the costs of chemicals, waste disposal, drilling, and labor. Each of these costs are directly affected by the requirements for the barrier and the strategy for design. The functional relationship between the total cost and the design variables is provided by the process model for the creation and reoxidation of the barrier.

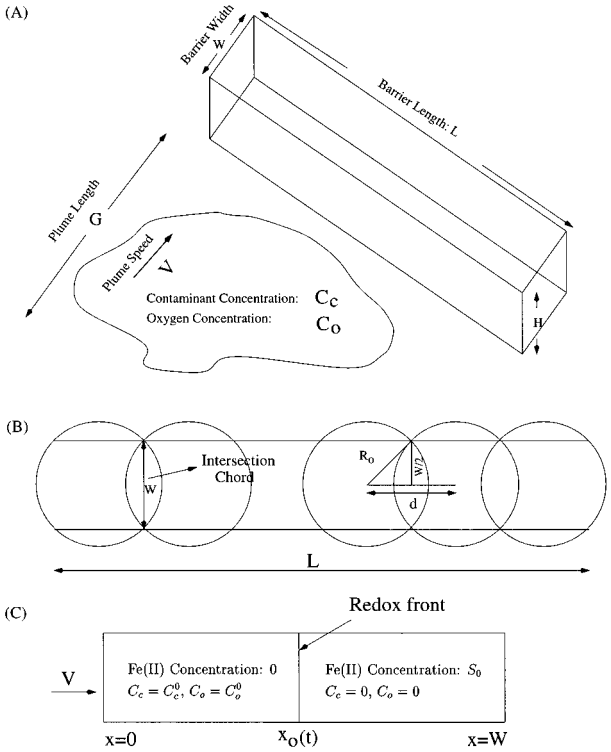

FIGURE 1. (A) Geometry of the barrier. (B) Barrier is created by overlapping the reduction zones from adjacent injections. (C) Transport-limited reoxidation of the barrier. All Fe(II) is consumed to the left of the redox front, and no contaminant/oxygen is present to its right.

Process Model

The process model consists of two parts: (a) the creation of the barrier through the injection of a dithionite solution and (b) the reoxidation of the barrier by the contaminant and any dissolved oxygen in the plume. The solution to the reoxidation submodel supplies the design criteria such as the width of the barrier to be established and the number of regenerations if any, whereas the solution to the reduction submodel determines the amount of the chemical reagent and the time duration of injection to establish a barrier of that width. A number of simplifying assumptions are made in each submodel in order to facilitate an analytic treatment of the problem.

Important among them is the assumption of physical and chemical homogeneity of the aquifer. Treatment of such heterogeneity is beyond the scope of the present work, although it represents a logical extension. The inevitability of field heterogeneity would require the use of numerical models and modification of the design guidelines obtained here, but the basic principles and approach remain the same. The homogeneity assumption allows the injection problem to be treated as radially symmetric and the reoxidation problem to be 1-D Cartesian along the width of the barrier. We further assume that diffusion is negligible. This is quite reasonable for the injection problem because of the strong advection fields. Also, the vertical influx of oxygen at Hanford is negligible for the reoxidation problem.

Creation of the Barrier. We consider a rectangular geometry for the barrier (Figure 1A) extending through the vertical extent H (m) of the aquifer with a porosity ϕ. The length L (m) of the barrier perpendicular to the average

ambient groundwater flow is chosen to match or exceed the lateral extent of the plume so that all of the plume may pass through the barrier. The dimensions of the required barrier are achieved here by a series of single-well injections. Other strategies such as dipoles (a pair of injection−extraction wells) and triplets (one injection and two extraction wells) are feasible but less attractive because they are operationally complex and can lead to the undesirable extraction of the injected dithionite. A pulse of dithionite solution at a concentration C_d (mol/m^3) is injected from fully penetrating injection wells. Because the regional flow at Hanford is negligible as compared to the well-induced flow, a circular Fe(III)-reduced zone of radius R_0 (m) is established by each injection well. The complete solution to the creation and the propagation of an Fe(II) zone around an injection well is known (*17*). The only results we use here are for the radius R_0 of the Fe(III)-free zone, the duration T (hours) of injection as functions of the injection rate Q (m^3/h), and the number of moles M of dithionite injected at the well:

$$R_0 = \sqrt{\frac{Q}{k_2 H\phi\pi}}\left[\ln\left(\frac{k_1}{k_1+k_2}+\frac{2k_1k_2M}{S_0Q(k_1+k_2)}\right)\right]^{1/2} \qquad Q < \frac{2k_1M}{S_0} \quad (5)$$

$$T = \frac{1}{Q}\left[\frac{M}{C_d} + H\phi\pi R_0^2\right] \quad (6)$$

The reducible Fe(III) content in the sediment is S_0 (mol/m^3). For large Q ($\geq (2k_1M/S_0)$), the contact time between dithionite and Fe(III)(s) would not be sufficient to allow the formation of an Fe(III)-free zone (i.e., $R_0 \equiv 0$). The distance between adjacent injection wells is chosen to yield the width of their intersection chord to be the desired width of the barrier (see Figure 1B). This ensures that a minimum redox capacity exists at any location along the length of the barrier, thereby preventing the passage of untreated plume during anytime between the regenerations of the barrier. A barrier of length L is established by using N_w wells as determined from $(N_w - 1)d = L$, where d is the separation distance for adjacent wells. It follows from simple geometry that the distance d between the wells is $d = \sqrt{4R_0^2 - W^2}$ and that

$$R_0 = \frac{1}{2}\left[\frac{L^2}{(N_w-1)^2} + W^2\right]^{1/2} \quad (7)$$

Combining eqs 5 and 7 and solving for M of dithionite needed at each well:

$$M = \frac{S_0Q}{2k_2}\left[\frac{k_1+k_2}{k_1}\exp\left\{\frac{k_2H\phi\pi}{4Q}(L^2/(N_w-1)^2 + W^2)\right\} - 1\right] \qquad \text{if } Q < \frac{2k_1M}{S_0} \quad (8)$$

It is easy to show that for a given radius R_0 (which gets fixed when N_r and N_w are chosen), M is strictly convex with Q and exhibits a minimum value. Because the cost of the dithionite reagent is significant, the injection rate Q becomes one of the key design variables in minimizing the total cost.

Reoxidation of the Barrier. A schematic of the reoxidation of the barrier is sketched in Figure 1C. The flow of groundwater is from left to right, along which the width of the barrier is W. Because the reoxidation reactions are very fast, both oxygen and Cr(VI) are immediately consumed upon contact with the barrier. This reaction occurs at the front, to the left of which all the Fe(II) is oxidized. To the right, Fe(II) is at its initial concentration S_0, which is the same as the reducible Fe(III) content. The front moves from left to right, and the lifetime of the barrier is when the front reaches the end of the barrier, thus using up all the Fe(II). Because the decrease in Fe(II) at the front is directly related to the number of moles of oxygen and Cr(VI) delivered to the front, the propagation of the front through the barrier is found by writing a mass balance for Fe(II) around the front. If the front moves a distance of Δx_0 during the time from t to $t + \Delta t$:

$$\underbrace{H\,L\,S_0\,\Delta x_0}_{\text{Decrease in Fe(II) at the front}} = \underbrace{H\,L\,V\,(F_cC_c + F_oC_o)\,\Delta t}_{\text{Fe(II) oxidized by the } O_2/Cr(VI) \text{ delivered at the front}} \quad (9)$$

Integrating between $x_0(t = 0)$ and $x_0(t = T_{barrier}) = W$ where $T_{barrier}$ is the time at which the barrier is completely oxidized:

$$T_{barrier} = \frac{WS_0}{V(F_cC_c + F_oC_o)} \quad (10)$$

Because the degradation of the contaminant is transport limited, the rate of cleanup of the plume is the rate at which it moves into the barrier. A plume of length G (which includes estimates of the source feeding the plume), moving at a speed V will have a total contact time with the barrier equal to G/V. So the minimum width W of the barrier for treating this plume has to be chosen such that $T_{barrier}$ in eq 10 equals G/V.

Regeneration of the Barrier. For long plumes, eq 10 would require a large W for $T_{barrier}$ to equal G/V. But a large W can be wasteful because in the creation of the barrier, the injected dithionite solution would have too great a travel time from the central injection well. A longer travel time allows a larger fraction of the dithionite reagent to undergo wasteful decay. A reasonable strategy to reduce this wastage is to generate a narrower barrier but periodically regenerate it near the end of its lifetime. Some of the reductive capacity is expected to be permanently lost upon each regeneration. Laboratory studies with Hanford sediments have shown this loss to be only about 5−10% (*5*) so that it is neglected here. For the conditions at Hanford, this loss represents a high estimate. This is because the column experiments employed faster flows (larger inertial forces that carry away dissolved Fe^{2+}) and higher dithionite concentrations (larger ionic strength decreases the adsorption of Fe^{2+}). Each regeneration of the total planned regenerations extend the life of the barrier by the time period $T_{barrier}$, and so we require that $T_{barrier} = (G/VN_r)$. Combining this with eq 10 yields the required width of the barrier using a regeneration approach as

$$W = \frac{G(F_cC_c + F_oC_o)}{S_0N_r} \quad (11)$$

Equation 11 is the key result that ties the reoxidation submodel to the reduction submodel by specifying the required width of the barrier that will be created N_r times.

Cost Model

A field implementation of the ISRM technology incurs costs associated with chemicals, drilling, labor/energy, and waste disposal. There are other costs such as field characterization and monitoring that are important but are not impacted by the design variables. For example, more monitoring wells might be needed for laterally extensive plumes, and more frequent monitoring might be needed for fast moving plumes.

The cost of drilling and well development, $\$_W$, is directly affected by the depth and the vertical spread of the plume as the barrier needs to intercept all of the plume. Dozens of wells are normally required, and so the economy of scale reduces the per well cost. The energy/labor cost of injection, $\$_L$, is expected to be proportional to the duration of the injection operation, apart from small fixed costs. As pointed

out earlier, periodic regeneration of the barrier can be advantageous in some cases. However, each regeneration incurs a cost, $\$_R$, for the remobilization of personnel and equipment.

While the other components of the cost are found in most field remediation efforts, the cost of injection chemicals, $\$_C$ is somewhat unique to the reactive barrier technology. At Hanford, each delivery unit of the injection chemicals consisted of about 5300 lb of sodium dithionite (and the pH buffers consisting of potassium carbonate/bicarbonate) and costing about $25 000, which works out to about $2 for each mole of dithionite. The main byproduct in the injection of dithionite solution is sulfate, which should be pumped out of the aquifer and disposed according to the regulatory requirements. The associated cost is quite variable depending on the amount/concentration of injected dithionite solution, the duration of pumping, and the cost of waste treatment if needed. The duration of pumping is often 5−10 times (depending on the heterogeneity of the formation) as long as the injection because of the need to ensure the removal of as much sulfate as possible. If the concentration of sulfate is low enough, it may be disposed at the local waste treatment plant at no cost. The water pumped from the well can also contain contaminated groundwater in addition to sulfate. This does not happen here with Cr(VI) but happens, for example, with TCE contamination because the reduction of TCE in the barrier occurs at a slower rate. The cost of waste disposal would be significantly higher if this happens. Because the amount of sulfate waste produced is directly proportional to the amount of dithionite injected, it is convenient to lump the sulfate disposal costs into the cost of dithionite. This makes the cost of chemicals range from a minimum of $2/mol of dithionite (with zero disposal costs) to $5 that allows for large waste disposal costs. On the basis of this discussion, a simple model for the total cost $\$_T$ is written as

$$\$_T = N_w\$_W + N_r\$_R + N_rN_w[\$_L T + \$_C M] \qquad (12)$$

Equations 6 and 8 give the functional form of T and M in terms of the barrier requirements and the design variables, thereby tying the cost and process models for the remediation operation.

Optimization

Using eqs 6, 8, and 11 in eq 12 yields an expression for the total cost, $\$_T$, that is a function of the design variables N_w, Q, and N_r. Because N_r and N_w are required to be integers we have a mixed-integer optimization problem. For some fixed values of N_w and N_r, the extremum in $\$_T$ occurs when

$$\frac{d\$_T}{dQ} \equiv N_r\,N_w\left[\$_L\frac{dT}{dQ} + \$_C\frac{dM}{dQ}\right] = 0 \qquad (13)$$

From eqs 5 and 11, it can be seen that fixing N_w and N_r fixes R_0. For fixed R_0 we can show from eqs 6 and 8 that (dM/dQ) changes sign from negative to positive as Q increases and that $(dT/dQ) < 0$ and $(d^2T/dQ^2) > 0$ for all Q. Thus, it follows that $d^2\$_T/dQ^2$ is strictly positive, guaranteeing a unique minimum for $\$_T$ for each fixed N_r and N_w. Because dT/dQ is always negative, dM/dQ has to be positive at the root Q^* of eq 13. So Q^* has to be greater than the Q that would minimize M alone. The minimum bound Q^*_{min} on Q^* is found by solving $dM/dQ = 0$:

$$Q^*_{min} = R_0^2\left[\frac{k_2 H\phi\pi}{1 + W_f\left(-\dfrac{k_1\exp(-1.0)}{k_1 + k_2}\right)}\right] \qquad (14)$$

where $W_f(\,)$ is the Lambert W function (*19*) that is evaluated on its principal branch where the value of $W_f(-(k_1\exp(-1.0)/k_1 + k_2))$ lies between 0 and −1, guaranteeing a positive value for Q^*_{min}. The upper bound on Q^* is $2\,k_1M/S_0$ because for $Q > 2k_1M/S_0$, $R_0 \equiv 0$. Because the root Q^* is unique with known bounds, solving $d\$_T/dQ = 0$ is very quick. The optimal set $\{N_r^{opt}, N_w^{opt}, Q^{opt}\}$ is chosen as the set that yields the least total cost over all the combinations of N_r and N_w:

$$\$_T(N_r^{opt}, N_w^{opt}, Q^{opt}) = \min_{N_w,N_r}\$_T(N_r, N_w, Q^*) \qquad (15)$$

The lower limits on N_w and N_r are 2 and 1, respectively. If $\$_T^*$ is the currently available minimum among all the combinations of $\{N_w, N_r\}$ searched so far, then the upper limits on N_w and N_r would simply be $\$_T^*/\$_W$ and $\$_T^*/\$_R$, respectively. So the enumeration in eq 15 is over a finite number of cases.

Even though there is an upper bound (equal to $2k_1M/S_0$) on Q^*, for some values of parameters this upper bound and the solution Q^* to eq 13 are still too large to be practical. While the maximum reasonable value for Q^* would be site specific (to avoid excessive mounding, fracturing, etc.), here we use 25 m^3/h (about 100 g/min) as the appropriate value at Hanford. That is

$$Q^* = \min\left(\text{solution to } \frac{d\$_T}{dQ} = 0 \quad 25\ m^3/h\right) \qquad (16)$$

The above truncation is only rarely triggered when long plumes (i.e., large G) are considered. Because of the monotonic decrease of $\$_T$ with increasing Q for $Q < Q^*$, the above truncation, even if triggered, would still give the least cost possible under the circumstances.

Figure 2 illustrates the mechanics of obtaining the optimal design variables for the base case problem with all parameters at their base case values as shown in Tables 1 and 2. All the site-specific data was obtained from the treatability studies conducted at the site during the period 1997−1999. Figure 2A plots $\$_T(N_r, N_w, Q^*)$ against N_w with N_r as a parameter, while Figure 2B plots Q^* against N_w with N_r as a parameter. Figure 2A identifies N_r^{opt} and N_w^{opt} whereas Figure 2B identifies Q^{opt}. Regeneration is not favored in this case as the least minimum cost ($4.33 million) is obtained with $N_r = 1$ and by using 38 wells with an injection rate of 12.89 m^3/h, operating for about 62.4 h. The width of the barrier would be about 11.9 m with a lifetime of about 18 yr. The adjacent wells are separated by about 13.5 m. The cost of chemicals and waste disposal accounts for over 85% of the total cost, drilling accounts for 9%, and labor accounts for 5%. As is the case here, we find that the dominant cost in general is the cost of chemicals and waste disposal.

Results and Discussion

In reality, the lifetime of the barrier is likely to be smaller than $G/(VN_r)$ due to presence of fast advective paths through the barrier that cause the barrier to be breached earlier. On the other hand, the design in Figure 1 is conservative because we do not assume credit for the reduction zone (with an Fe(III) reduction of less than 100%) established beyond W. While it is beyond the scope of this paper to quantify, it can be argued that the additional redox capacity created beyond W will help mitigate the adverse of effects of heterogeneity. The simplifying assumptions employed here mean that the optimal design strategy obtained here is really a guideline for developing a more sophisticated field design that accommodates heterogeneity.

It follows from the Reoxidation of the Barrier section that the required width W of a barrier is primarily a function of the iron content in the sediment and the mass of oxygen and contaminant in the plume. For low iron content and/or high

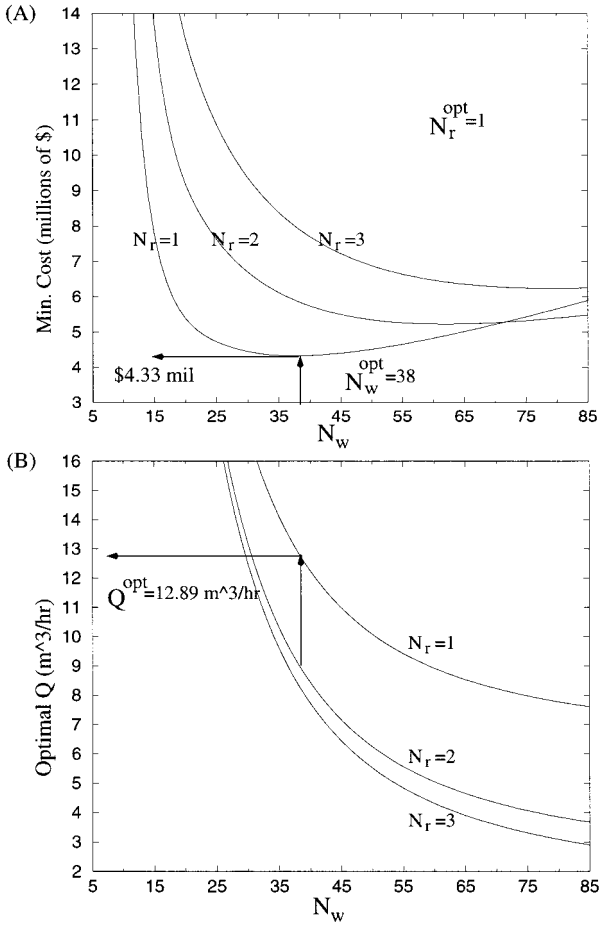

FIGURE 2. Optimal design variables are obtained by obtaining the optimum *Q* for a range of values for N_r and N_w and picking the (N_r, N_w, *Q*) combination with the least minimum cost.

contamination, larger width would be needed. For Cr(VI) contamination at Hanford, the required width W is much smaller than the length L of the barrier. The barrier is created as in Figure 1B by overlapping circular reduction zones of radius R_0, which is always greater than $W/2$ according to eq 8. While the creation of the circular reduction zone with R_0 much bigger than $W/2$ might require fewer wells, an excessive amount of dithionite would also be wasted because reducing beyond the required width W is unnecessary. Also, the longer travel time to get to a large distance R_0, from the injection, contributes to the wastage of dithionite due to disproportionation. Because the cost of chemicals and waste disposal is dominant, R_0 and W are generally about the same magnitude at the optimal configuration. For example in Figure 2, R_0 is about 9.0 m whereas W is 11.9 m. Reworking the same problem with the chemical cost at $2 (the least possible value considered here), we still get the optimal N_r as 1 (thus fixing W at 11.9 m), but R_0 increases marginally to 9.46 m with about 80% of the total cost going toward chemicals. Increasing all other costs to their highest values while holding the chemical cost at its smallest value ($2), we again get $N_r^{opt} = 1$ and $W = 11.9$ m, but R_0 increases to 10.24 m with about 70% of the total cost for chemicals. The important conclusion here is that when the chemical costs are dominant, the distance of separation between adjacent wells is strongly correlated with the width of the barrier so that the desired length of the barrier can only be obtained by increasing the number of wells.

Because the radius of the reduction zone is controlled by W, W is the key factor in determining the injection rate Q, whereas both W and L are key factors impacting the selection of N_w. W can however be decreased by opting for regeneration, i.e., using $N_r > 1$, because W is inversely proportional to N_r. As discussed in the Reoxidation of the Barrier section, regeneration would be favored for large W due to the wastage of chemicals. However, as we have just seen in the previous paragraph, any decrease in W would also decrease the distance of separation between adjacent wells so that the number of wells required to build the barrier will go up. This is seen in Figure 2 where the optimal number of wells increase from 38 to 62 as N_r increases from 1 to 2 and from 62 to 80 as N_r is further increased to 3. When N_r doubles, the required width W is halved, which in turn approximately halves the distance between the wells, leading to the approximate doubling of the number of wells required for a barrier of specified L. Likewise, Figure 2 indicates that the optimal Q has an approximate inverse relation with N_r^2. Thus, the cost savings in the decreased wastage of chemicals has to be weighed against the increased drilling and labor/energy costs when considering regeneration. The differential cost of increasing N_r, i.e., $d\$_T/dN_r$ is much larger than $d\$_T/dN_w$ (as can be also be estimated from Figure 2A) so that N_r^{opt} is usually in single digits while N_w^{opt} can be much larger.

The uncertainties in the unit cost estimates as indicated in Table 2 have a small impact on the optimal design strategy for the base case. The optimal design strategy for the base case is to employ 38 wells at an injection rate of 12.9 m^3/h and with no regenerations (i.e., $N_r^{opt} = 1$). As the cost estimates are varied, N_r^{opt} is unchanged at 1, whereas the response of Q^{opt} is opposite to that of N_w^{opt}. The sensitivity is small however with N_w^{opt} varying between 35 and 39 and Q^{opt} varying between 11.9 and 14.9 m^3/h. Because N_r^{opt} ($\equiv 1$) fixes W, R_0 and thus Q^{opt} and N_w^{opt} are controlled tightly. Increasing chemical costs force R_0 to be closer to W in order to reduce the wastage of chemicals, and the smaller R_0 in turn requires smaller Q but more injection wells. Increasing drilling costs decrease N_w^{opt}. An increase in labor/energy costs increases Q^{opt} so that the operational time T may be decreased. This is accompanied by a decrease in N_w^{opt} because a larger injection rate can increase R_0 and the well separation distance. The role of different costs in making up the overall cost is studied by considering 256 (four values each for the four cost estimates yielding 4^4 cases) possible cases. On the average, the cost of chemicals turns out to be dominant making up about 84.3% of the total cost, followed by drilling (8.9%), labor (5.6%), and regeneration (1.2%) costs. The dominance of chemical costs has important implications to the overall optimal design strategy so that it is examined closely in the next section.

Analysis of Chemical Costs. The observed dominance of chemical costs allows the cost model to be simplified to develop insights into the cost-effectiveness of the design. When all other costs are negligible as compared to chemical costs, the total cost can be minimized by operating each well at some optimal Q to minimize the wastage of chemicals. The minimum number of moles of dithionite needed to establish a reduction zone of radius R_0 is derived by minimizing M in eq 8 with respect to Q. Q_c^{opt} is unique and is given by eq 14. Variables with a subscript "c" are used in this section to imply that they apply to the special case of considering chemical costs alone. Using eq 14 in eq 8 yields the minimum M at each well and during each injection campaign. Multiplying that with N_{rc} and N_{wc} yields the total number of dithionite moles M_c^T needed for remediation when each well is operating to minimize the wastage of dithionite. The optimal N_{rc} and N_{wc} are now picked by

TABLE 1. Definition and Description of Process Model Parameters

parameter	description	value (for the test site at Hanford), U
L, W, H, ϕ	length, width, height, and porosity of barrier	$L = 500$ m, $H = 15$ ft (4.572 m), $\phi = 0.14$
V	speed of plume	1 ft/day (0.3048 m/day)
C_d	concn of dithionite in injection soln	50.0 mol/m^3
C_c, C_o	chromate/oxygen concns in plume	1 mg/L (0.019 mol/m^3) and 8 mg/L (0.25 mol/m^3)
F_c, F_o	no. of mol of Fe(II) oxidized by 1 mol of Cr(VI) and 1 mol of O	3 and 4
S_0	reducible Fe(III) content of barrier sediments	11.0e^{-6} mol/(g of sediment) or 177.57 mol/m^3 of pore space
k_1, k_2	rate constants for reduction of Fe(III) and disproportionation of dithionite	0.14, 0.04/h

TABLE 2. Definition and Description of Variable Parameters

parameter	description	values[a]
G	length of plume	1, *2*, 3, 4, 5, 6, 7, 8, 9, 10 km
$C	cost of chemicals and waste disposal per mol of dithionite	2, *3*, 4, 5 $/mol
$L	cost of energy and labor	50, *100*, 150, 200 $/h
$W	cost of drilling and well development	5K, *10K*, 15K, 20K $/well
$R	cost of regeneration	25K, *50K*, 75K, 100K $/regeneration

[a] The base case values are italic.

minimizing M_c^T. Using eqs 7 and 11 in the above and invoking $(N_{wc} - 1) \approx N_{wc}$, we get upon simplification

$$M_c^T \approx Z_1\left[\frac{L^2}{(N_{wc}/N_{rc})} + \left(\frac{G(F_cC_c + F_oC_o)}{S_0}\right)^2 (N_{wc}/N_{rc})\right] \quad (17)$$

where Z_1 is a process constant that is independent of the design variables. Clearly, M_c^T is a function only of the ratio N_{wc}/N_{rc} with a unique minimum. Solving $dM_c^T/d(N_{wc}/N_{rc}) = 0$ for the ratio $N_{wc}^{opt}/N_{rc}^{opt}$ and using it in eqs 7 and 14, we get the optimal design as the following. Each of the three quantities on the left below are seen to be independent of the design variables, which explains the linear variation of N_w^{opt} and the inverse square variation of Q^{opt} with N_r:

$$\frac{N_{wc}^{opt}}{N_{rc}^{opt}} = \frac{LS_0}{G(F_cC_c + F_oC_o)} \quad (18)$$

$$Q_c^{opt}(N_{rc}^{opt})^2 = \frac{k_2H\phi\pi G^2(F_cC_c + F_oC_o)^2}{2S_0^2\left(1 + W_f\left(-\frac{k_1\exp(-1.0)}{k_1 + k_2}\right)\right)} \quad (19)$$

$$(M_c^T)_{min} = \frac{H\phi\pi GL(F_cC_c + F_oC_o)}{4\left(1 + W_f\left(-\frac{k_1\exp(-1.0)}{k_1 + k_2}\right)\right)}\left[\frac{k_1 + k_2}{k_1}\exp\left\{1 + W_f\left(-\frac{k_1\exp(-1.0)}{k_1 + k_2}\right)\right\} - 1\right] \quad (20)$$

It is interesting to note that the above optimal solution corresponds to the situation where the distance between the adjacent wells is identical to the width of the barrier.

The extent to which eqs 18−20 do not predict the optimal operational strategy is a measure of its sensitivity to the costs of drilling, labor, and regeneration. Figure 3A examines this for the Cr(VI) contamination at Hanford. The three quantities N_w^{opt}/N_r^{opt}, $Q^{opt}(N_r^{opt})^2$, and M^T, and the corresponding ratios with respect to the theoretical estimates from eqs 18−20 are computed for all 256 cases. If the fractional cost of chemicals is unity, then each of these ratios would be exactly unity. Figure 3A plots the three ratios against the fractional cost of chemicals. As expected $(M^T)_{min}$ is always larger than $(M_c^T)_{min}$ but is only about 12.5% larger in the worst case when the fractional cost of chemicals is at a minimum. All three ratios tend toward unity as the fractional cost of chemicals increases. The consideration of drilling costs is expected to decrease the number of wells, whereas the consideration of the labor/energy costs is expected to decrease the duration of injection, i.e., increase the injection rate. This is exactly what is observed in Figure 3A where eq 19 determines a lower bound on $Q^{opt}(N_r^{opt})^2$ and eq 18 determines the upper bound on N_w^{opt}/N_r^{opt}.

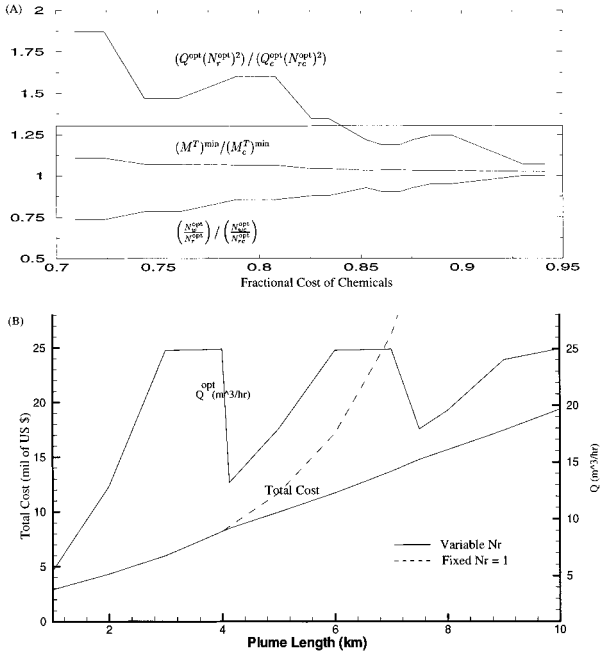

FIGURE 3. (A) Effect of considering labor, drilling, and regeneration costs on the optimal strategy that minimzes the chemical costs alone. (B) Periodic regeneration of the barrier becomes attractive for long plumes.

Case for Regeneration. While the base case considered here does not favor regeneration, long plumes (large G) and/or sediments with small treatment capacity (small S_0) can increase the required width of the barrier according to eq 11, where regeneration becomes attractive. Because of the uncertainties in Cr(VI) source feeding the plume, G is varied over a range of values from 1 to 10m to determine the impact on design strategy. Figure 3B shows that the total cost of the

operation would be much larger if regeneration is not considered (i.e., N_r held at 1). As G increases, N_r^{opt} jumps to 2 when the plume is over 4.125 km long and to 3 when the plume is 7.5 km long. While N_r is unchanged (e.g., for G between 1 and 4km), Q^{opt} increases because W increases with G. When N_r makes a discrete jump, both W and Q^{opt} decrease abruptly. This is followed by a steady increase until N_r jumps once again. The increase in Q^{opt} is large enough that the truncation in eq 16 is triggered, which caps Q^{opt} at 25.0 m^3/h.

Literature Cited

(1) Powell, R. M.; Puls, R. W.; Blowes, D. W.; Vogan, J. L.; Gillham, R. W.; Schultz, D.; Powell, P. P.; Sivavic, T.; Landis, R. *Permable reactive barrier technologies for contaminant remediation*; Technical Report; EPA/600/R-98/125; Office of Research and Development, Office of Solid Waste and Emergency Response, U.S. EPA: Washington, DC, 1998.

(2) Agrawal, A.; Tratneyak, P. G. *Environ. Sci. Technol.* **1996**, *30*, 153−160.

(3) Blowes, D.; Ptacek, C.; Jambor, J. *Environ. Sci. Technol.* **1997**, *31* (12), 3348−3357.

(4) Sivavec, T.; Mackenzie, P.; Horney, D.; Baghel, S. *Redox-active media for permeable reactive barriers*; Technical Report; General Electric Research and Development Center: Schenectady, NY, 1996.

(5) Szecsody, J. E.; Fruchter, J. S.; Sklarew, D. S.; Evans, J. C. *In situ redox manipulation of subsurface sediments form Fort Lewis, Washington−Iron reduction and TCE degradation mechanisms*; Technical Report; Pacific Northwest National Laboratory: Richland, WA, 2000; PNNL Report 13178.

(6) Sass, B. M.; Rai, D. *Inorg. Chem.* **1987**, *26*, 2228−2232.

(7) Patterson, R. R.; Fendorf, S.; Fendorf, M. *Environ. Sci. Technol.* **1997**, *31* (7), 2039−2044.

(8) Puls, R. W.; Paul, C. J.; Powell, R. M. *Appl. Geochem.* **1999**, *14*, 989−1000.

(9) Amonette, J. E.; Szecsody, J. E.; Schaef, H. T.; Templeton, J. C.; Gorby, Y. A.; Fruchter, J. S. Abiotic reduction of aquifer materials by dithionite: A promising in-situ remediation technology. In *In Situ Remediation: Scientific Basis for Current and Future Technologies*; Gee, G. W., Wing, N. R., Eds.; Battelle Press: Columbus, OH, 1994; pp 851−881.

(10) Istok, J. D.; Amonette, J. E.; Cole, C. R.; Fruchter, J. S.; Humphrey, M. D.; Szecsody, J. E.; Teel, S. S.; Vermeul, V. R.; Williams, M. D.; Yabusaki, S. B. *Ground Water* **1999**, *37* (6), 884−889.

(11) Williams, M. D.; Vermeul, V. R.; Szecsody, J. E.; Fruchter, J. S.; Cole, C. R. *100-D area in situ redox treatability test for chromate contaminated groundwater: FY 1998 year-end report*; Technical Report; Pacific Northwest National Laboratory: Richland, WA, 1999; PNNL Report 12153.

(12) Williams, M. D.; Vermeul, V. R.; Oostrom, M.; Evans, J. C.; Fruchter, J. S.; Istok, J. D.; Humphrey, M. D.; Lanigan, D. C.; Szecsody, J. E.; White, M. D.; Wietsma, T. W.; Cole, C. R. *Anoxic plume attenuation in a fluctuating water table system: Impact of 100-D area in situ redox manipulation on downgradient dissolved oxygen concentrations*; Technical Report; Pacific Northwest National Laboratory: Richland, WA, 1999; PNNL Report 12192.

(13) Williams, M. D.; Oostrom, M. *J. Hydrol.* **2000**, *230* (1−2), 70−85.

(14) Eary, L.; Rai, D. *Environ. Sci. Technol.* **1988**, *22*, 972−977.

(15) Fendorf, S. E.; Zasoski, R. J. *Environ. Sci. Technol.* **1992**, *26*, 79−85.

(16) White, M. D.; Oostrom, M. *STOMP 2.0: Subsurface Transport Over Multiple Phases, Theory Guide*; Technical Report; Pacific Northwest National Laboratory: Richland, WA, 1999; PNNL Report 12030.

(17) Chilakapati, A. *AIChE J.* **1999**, *45* (6), 1342−1350.

(18) Corless, R. M.; Gonnet, G. H.; Hare, D. E. G.; Jeffrey, D. J. *On the Lambert's W function*; University of Waterloo: Waterloo, Canada, 1993; Technical Report CS-93-03.

Received for review January 21, 2000. Revised manuscript received September 25, 2000. Accepted September 25, 2000.

ES000920H